THE ASTROPHYSICAL JOURNAL, 300:624–638, 1986 January 15

Hα VELOCITY WIDTHS OF GIANT EXTRAGALACTIC H II REGIONS

JEAN-RENÉ ROY,[1,2,3] ROBIN ARSENAULT,[1,3] AND GILLES JONCAS[4]

Received 1985 May 20; accepted 1985 July 17

ABSTRACT

Integrated Hα line profiles of 47 giant extragalactic H II regions have been obtained with a Fabry-Perot spectrometer. The observed H II regions belong to 16 nearby late-type spirals and Magellanic irregulars. A relationship of the form $D \propto W^n$ is found between the linear diameters, D, of the H II regions and the velocity width, W, of the profile in excess of the thermal broadening, confirming a trend discovered by Melnick (1977) from a much smaller sample of objects. The shape of the relation is dependent on the adopted distances to the galaxies. The power index n is found to be smaller than 1.6, which is inconsistent with virialized motions in a gravitationally bound system. The mean velocity width $\langle W \rangle$ of the three largest H II regions is strongly correlated with the absolute magnitude of the parent galaxy. Quality of fits for different distance scales to the galaxies is discussed. Models based on stellar winds, champagne flows, and self-gravitation are briefly discussed, and hydrodynamic turbulence is suggested as the most viable mechanism to explain the observed relationships between velocity dispersion, H II region diameter, and galaxian absolute magnitude. The similar behaviors of velocity dispersion as a function of linear size, L, observed in two galactic H II regions (M17 and S142) and in giant extragalactic H II regions, indicates that a relationship of the form $W \propto L^{0.3}$ may apply over nebular scales ranging from 1 to 1000 pc.

Subject headings: galaxies: internal motions — nebulae: H II regions

I. INTRODUCTION

Giant star-forming complexes are relatively luminous objects in galaxies. This makes their observation feasible with high resolution spectroscopic techniques and allows one to study the chemistry, the kinematics, the dynamics, and the process of star formation in late-type galaxies. The intrinsic properties of the so-called giant extragalactic H II regions have received much attention from radio and optical astronomers. There is no precise definition of a giant extragalactic H II region; if a linear size greater than about 100 pc can be defined for what appears to be an isolated nebula, it qualifies in principle for the title; the largest among these objects, such as 30 Dor in the Large Magellanic Cloud or NGC 5471 in M101, have diameters reaching several hundred parsecs. While it is unlikely that any analog to 30 Dor or to NGC 5471 will be found in our own Galaxy, which is consistent with the morphology of the Milky Way, Kennicutt (1984) has shown that the physical properties of the largest H II regions merge with those of the less luminous giant H II regions, including the largest galactic objects, such as the Carina nebular complex, NGC 3603, and W49. Apart from their gigantic size, an important physical property makes giant H II regions distinct from the more familiar and smaller galactic H II regions: it is their large velocity dispersion. Indeed, every kinematic study, using either Fabry-Perot spectrometer scans or echellograms (Smith and Weedman 1972; Melnick 1977; Gallagher and Hunter 1983; Rosa and Solf 1984; Skillman and Balick 1984), leads to the inescapable result that gas motions in giant H II regions reach supersonic velocities equivalent to Mach 2 or 3.

In a stimulating series of papers, Melnick (1977, 1978, 1979, 1980) and Terlevich and Melnick (1981) presented results of Fabry-Perot spectroscopy and photometry of about 20 giant H II regions from several nearby galaxies. A particularly important result was the very strong correlation found between the velocity width in excess of thermal motion and the linear diameter and the luminosity of giant H II regions. Because of the known relationship between the absolute magnitude of a galaxy and the average diameter of its largest H II regions (Sérsic 1960; Sandage 1962; Kennicutt 1979*b*), the velocity width of a particular emission-line profile could turn out to be a more reliable distance indicator than the elusive diameter. Calibrations of velocity dispersion as a distance indicator were attempted by Melnick (1978) and by de Vaucouleurs (1979*c*). However, Gallagher and Hunter (1983) failed to find the above correlation between velocity width and diameter in their study of 28 H II regions belonging to a set of dwarf Magellanic irregulars and related galaxies. Their observations were done with an echelle spectrograph providing about the same spectral resolution as the Fabry-Perot work, with the convenience of spatial resolution along the slit. Their study shows a trend of increasing velocity width with increasing diameter only for the few "supergiant" H II regions having sizes greater than 500 pc. Gallagher and Hunter emphasize the fact that their sample is less homogeneous than Melnick's; however, their conclusions throw serious doubt on the relation found by Melnick and Terlevich.

The frailness of the possible relation between velocity width and diameter of H II regions is not unexpected. Several reasons contribute to the uncertainties: (1) the sizes of the samples are small; (2) some linear diameters are based on eye estimates of angular diameters which are known to be sometimes unreliable (Kennicutt 1979*a*); (3) the sizes of field stop used by observers differ and could introduce a varying degree of blending from nearby regions; (4) the inference of a linear diameter depends on an accurate knowledge of the distance to the galaxy. The

[1] Département de physique, Université Laval, and Observatoire astronomique du mont Mégantic.
[2] Anglo-Australian Observatory.
[3] Visiting Astronomer, Canada-France-Hawaii Telescope, operated by the National Research Council of Canada, the Centre National de la Recherche Scientifique of France, and the University of Hawaii.
[4] Observatoire de Marseille.

fundamental uncertainties on the last probably have the strongest effect.

Different mechanisms have been proposed to explain the energy sources powering the supersonic motions in giant extragalactic H II regions: self-gravitation (Terlevich and Melnick 1981), stellar winds (Dyson 1979), champagne flows (Tenorio-Tagle 1979; Rosa and Solf 1984), and hidden supernovae (Skillman and Balick 1984). Most of these mechanisms make some prediction about the slope of the relationship between velocity and linear size.

This paper presents the results of a study of velocity dispersions in giant extragalactic H II regions. Velocity dispersions were deduced from Hα profiles obtained with a Fabry-Perot spectrometer in 47 giant H II regions observed in 16 nearby spiral and irregular Magellanic galaxies. We confirm the trend found by Terlevich and Melnick (1981). However, we find a much weaker correlation between velocity dispersion W and size D; moreover, the slope of our relation is less steep than theirs by at least 0.25 in the (log D, log W)-plane. Although some differences can be explained by our much larger sample and by our more rigorous technique of deconvolution of the observed line profile, the shape of the relationship is found, not surprisingly, to be most sensitive to the adopted distances to the target galaxies.

II. OBSERVATIONS

The Hα line profiles of giant H II regions were obtained with a large-aperture Fabry-Perot spectrometer using a servo-stabilized, piezoelectrically scanned interferometer. The instrument and several examples of observations are presented in Arsenault and Roy (1984). The free spectral range of the interferometer at Hα is 0.62 nm (283 km s^{-1}), and the FWHM corresponds to 0.46 nm (21 km s^{-1}), for a spectral resolution of approximately 15,000. The detector is a GaAs photomultiplier (RCA C31034). Control of the scanning and data acquisition are achieved with an HP-85 microcomputer. An interference filter with its transmission peak centered at the redshifted wavelength of the nebular line acts as a premonochromator to reject the unwanted orders. An observing sequence is the sum of several repetitive scans covering two successive orders of interference, with typically 1–5 s of integration per step. A line-profile observation is terminated when the maximum number of counts reaches about 400. Calibration scans of the Hα line from a Plucker discharge tube were taken before and after each observation in order to check the stability of the interferometer and to provide a zero point for the radial velocity scale.

The observations were done on the 1.60 m f/8 telescope of the Observatoire astronomique du mont Mégantic and on the 3.60 m f/8 of Canada-France-Hawaii telescope on Mauna Kea. The entrance aperture of the spectrometer corresponded to 48″ and 21″ on the sky, respectively, on these telescopes. Since most H II regions have angular sizes ranging from 5″ to 20″, the aperture used was sufficiently large to accept the total light from most of the observed H II regions. We tried to select isolated objects, but there are a few cases where contamination by nearby objects could have affected the profiles of the target H II regions; we have supposed the galaxian diffuse Hα emission to be negligible compared with that of the H II region. Astrometric positions good to 2″–5″ were kindly supplied to us by R. C. Kennicutt for a large number of objects; other positions came from Israel, Goss, and Allen (1975) and from Israel (1980). Several objects were observed twice in order to check the consistency of our results. Table 1 lists the galaxies observed and the number of H II regions observed in each galaxy.

III. DATA REDUCTION

The observed profile of a nebular spectral line is a convolution of the instrumental profile with a Gaussian describing the thermal broadening in the H II region and with a Gaussian Doppler profile representing the velocity field of the nebula. This velocity field includes turbulence, expansion, rotation, relative motions of isolated cells, and so on. It is a complicated task to disentangle the various kinematic components from projection smearing (Scalo 1984). Fortunately the observed velocity profile is generally quite accurately described by one Gaussian function ($\exp[-(V-V_0)^2/W^2]$); V_0 is the radial velocity, and W is the e-folding width that we call "velocity width." Examples of observed Hα profiles of giant H II regions are shown in Figure 1. Line profiles of giant H II regions obtained with spatial resolution show complicated structures (Rosa and Solf 1984; Skillman and Balick 1984). Although several profiles obtained with our Fabry-Perot spectrometer show obvious asymmetry, which suggests that a better fit would be achieved with two or three Gaussians (Fig. 1*c*), we have assumed for the purpose of this paper a single Gaussian Doppler profile. Generally, the Hα line profiles integrated over whole H II regions are symmetrical; they have moderate velocity width and show little evidence of multiple kinematical components. Integrated profiles do not reveal the details of the internal kinematics, but they relate more easily to other large-scale properties of H II regions and galaxies. A forthcoming paper will examine the fine structure of the individual line profiles and will list several other parameters of the H II regions (position, radial velocity, etc.).

To reduce by as much as possible the uncertainty on the velocity width deduced from the observed profile, we paid close attention to the removal of accurate instrumental and thermal broadening profiles. The instrumental profile of the spectrometer was established by measuring the heavy-ion Ne 659.5 nm line from a calibration lamp for several sizes of the entrance diaphragm; the instrumental function was well represented by a Lorentzian. Because of the multiple components forming the Hα line, its intrinsic width is larger than that of the Ne 659.5 nm line; using the heavy-ion line results in a slight overestimate of the calculated velocity width. This is, however, smaller than the other uncertainties on the velocity width. For each H II region, the instrumental profile was taken to be that given by the diaphragm having the same angular size on the sky as the H II region. This is important because most giant H II regions did not fill the entrance aperture of the spectrometer; therefore, deconvolving with an instrumental function characteristic of the whole aperture would underestimate the width of the observed profile (cf. Flynn 1966); for the smallest (in angular size) H II regions, this can make a difference of several km s^{-1} in the deduced velocity width. A majority of the values of angular diameters of giant extragalactic H II regions were taken from Kennicutt (1978); they correspond to the diameter defined by the solid angle enclosing all isophotes brighter than 5×10^{-16} ergs cm^{-2} s^{-1} $arcsec^{-2}$. This isophotal level was chosen because it gives diameters close to those obtained from eye estimates. The night-sky Hα line was very faint compared with the brightness of the typical giant H II regions that we observed. Because the night-sky line was below the noise level for profiles of extragalactic objects whose

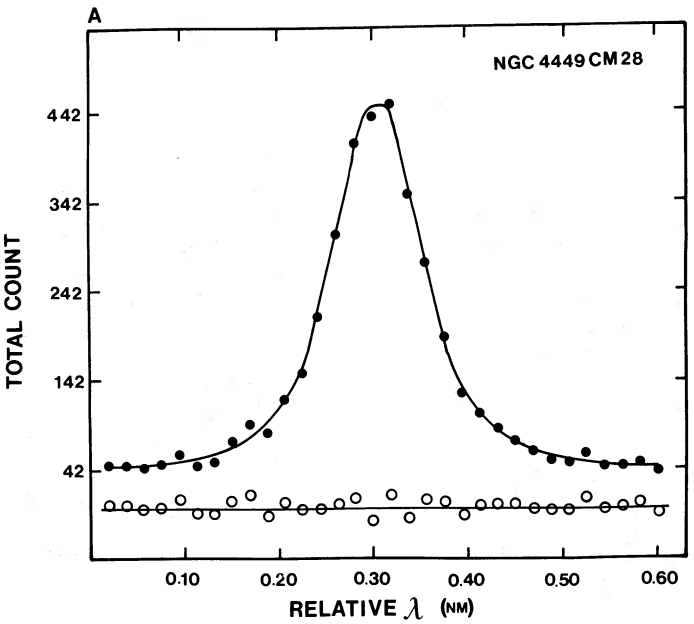

FIG. 1*a*

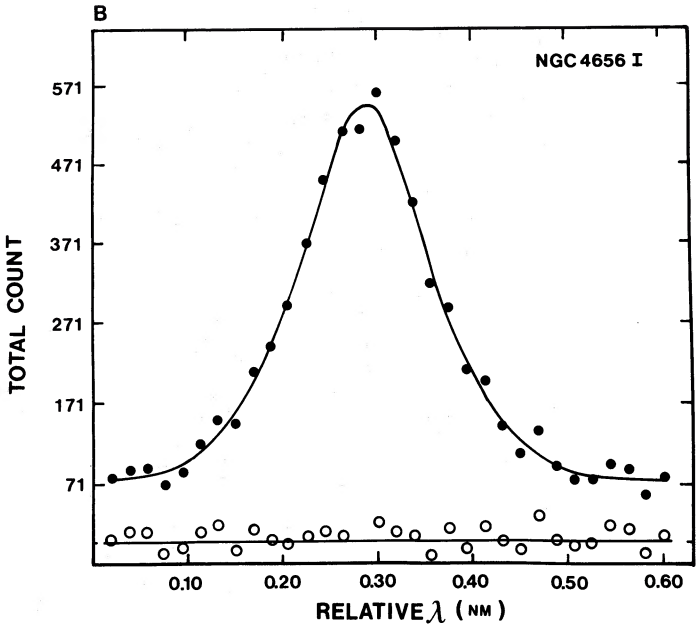

FIG. 1*b*

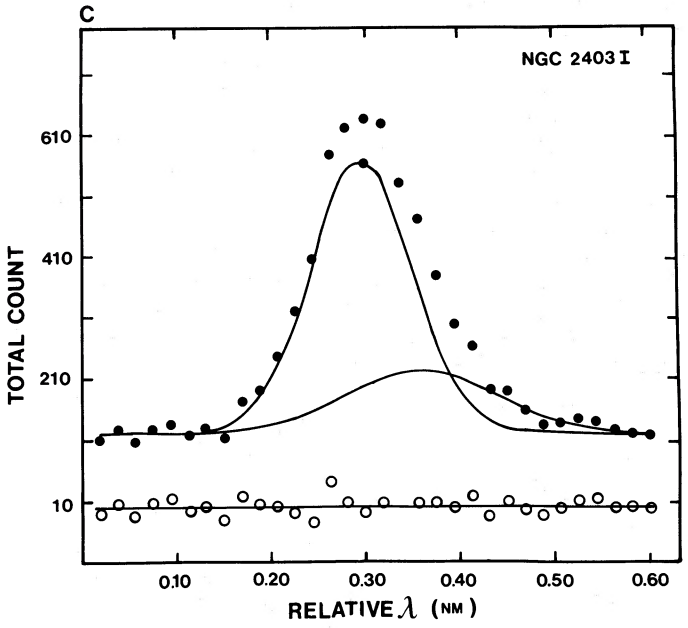

FIG. 1*c*

FIG. 1.—Examples of integrated Hα line profiles of giant extragalactic H II regions. The full line represents the best-fitted Voigt profile (Gaussian profiles for velocity and thermal broadening; Lorentzian profile for instrumental response of the Fabry-Perot spectrometer). The dots are the observed points, and the open circles are the residuals; the horizontal bar defines the zero level. (*a*) NGC 4449cm28 is representative of a region with a small velocity width of 20.0 ± 1.0 km s^{-1}; (*b*) NGC 4656 I is a region with a very large velocity width of 36.3 ± 1.2 km s^{-1}; (*c*) NGC 2403 I is an example of a giant H II region where the asymmetrical profile suggests a better fit with two velocity Gaussians.

redshift separated them from the terrestrial Hα line, we made the assumption of no line emission contribution from the night sky.

It is more difficult to take into account thermal broadening, because few extragalactic H II regions have had their temperature determined. Measurements of the temperature-sensitive ratios of [O III] and [N II] lines are made difficult by the very weak intensity of the [O III] 436.3 nm line and by the generally low intensity of the [N II] lines in the arms of spirals or in irregulars. Electron temperatures are known to vary by a few thousand degrees (e.g., Rayo, Peimbert, and Torres-Peimbert 1982); this corresponds to an uncertainty of 1–2 km s^{-1} in the deduced velocity width. We found from the literature (e.g., McCall 1982) electron temperatures determined by the [O III] line ratio for 14 of our giant H II regions. For seven more objects we used the empirical calibration of the line ratio [O III λ500.7]/Hβ, known as the excitation parameter, to infer electron temperatures. Several investigations have shown the validity of this approach (cf. Stasińska *et al.* 1981). The mean temperature for the above 21 H II regions is 10,250 (±2560) K. Therefore, in the case of the remaining 26 H II regions for which no spectrophotometric data were available, we assumed a temperature of 10,000 K. Values of the temperatures as well as the velocity widths of the Hα profiles of the giant extragalactic H II regions are listed in Table 2.

For 15 objects in common with Melnick (1977), the velocity widths agree to within 20%, except for the H II regions NGC 2403 III and NGC 5461, where differences of more than 30% (well beyond the instrumental errors and differences in data reduction) are obvious; there could be a problem of misidentification for these objects, or of the telescope pointing to slightly different parts of the H II complex. In addition, the projected sizes of diaphragms that we used (21″ and 48″) were smaller than the 62″ field stop used by Melnick. Other discrepancies possibly arise from the way the aperture effect was taken into account in the deconvolution of the observed profiles.

IV. LINEAR DIAMETERS OF GIANT EXTRAGALACTIC H II REGIONS

The measurement of extragalactic H II region diameters and their use as distance indicators has been discussed in depth by Kennicutt (1978, 1979*a*, *b*, *c*, 1981). Fairly accurate isophotal diameters can be obtained for a large number of extragalactic

H II regions. As stated earlier, we have used the diameters established by Kennicutt (1978) for a majority of the H II regions of this work. For the remaining objects, not included in Kennicutt's study, optical sizes were taken from Israel (1980) and other sources (cf. Table 2). As explained below, this last set of angular diameters will turn out to be less reliable.

To calculate the linear diameters of the H II regions, the distance to each parent galaxy must be known. Present distance determinations suffer from dramatic discrepancies. Even membership in specific groups is questionable. To rationalize our approach, we chose from the literature two sets of distances, each constructed with a fair degree of self-consistency, which include almost all of the galaxies of our H II region program. Although the distance to a particular galaxy may not be accurately known, the relative distances within each set of galaxies were assumed to be consistent within the framework of the methodology of each distance scale. We opted for the sets of distances given by Richter and Huchtmeier (1984, hereafter RH) and by Bottinelli *et al.* (1984, hereafter BGPV). With the help of evolved bootstrapping procedures, these two investigations have used the 21 cm line widths of the deprojected galaxies via the *B* band Tully-Fisher relation (Tully and Fisher 1977) to calibrate and derive the distance moduli of a large number of galaxies. Not surprisingly, distances derived in these two independent studies differ because of well-known differences in strategy in correcting for extinction, deprojecting for face-on views, and accounting for internal velocity dispersion in low-mass galaxies. It is not our task to attempt a critical analysis of these two works, but it is hoped that our investigation will clarify some points. NGC 3938, NGC 5194, and NGC 6822 were not used by RH because of the large uncertainty on their inclination, which introduces too large an error in calculating the corrected width of the 21 cm line profile. Since RH are close in their methodology and results to the "long" distance scale, we have selected distance moduli from the parameters listed by Sandage and Tammann (1981) for those galaxies. Table 1 lists the distance moduli of the galaxies observed as deduced from RH and BGPV. For comparison, we have added distance moduli from de Vaucouleurs (1979*a*, *b*, hereafter dV79*a*, *b*) which were derived from primary, secondary and tertiary indicators (see also de Vaucouleurs 1978). The sample of de Vaucouleurs does not contain all the galaxies of our study, but it includes those with probably the best distance determinations. Distances were used to convert the angular diameters of H II regions into linear diameters (Table 2). The reader should be aware that the number of significant figures for the diameters of the H II regions listed in Table 2 should be taken with a "pinch of salt."

V. VELOCITY-WIDTH RELATIONSHIPS

We have used the velocity widths deduced from the observed Hα profiles to construct sets of figures where the velocity widths (log W) of giant H II regions are related to other physical parameters. Each set of figures corresponds to each adopted distance set (RH, BGPV, or dV79*a*, *b*). First we plot the diameter (log D) as a function of the velocity width (log W) of the giant H II regions, with one graph for each distance scale. The results are shown for the distances of RH in Figure 2 and for the distances of BGPV in Figure 3. Figures 4–6 display the (corrected) absolute blue magnitude M_B of the parent galaxy deduced from RH, BGPV, and dV79 as a function of log $\langle W \rangle$, where $\langle W \rangle$ is the mean of the three largest velocity widths in each galaxy; these also correspond to the three largest H II regions. The straight lines are the linear regressions fitted through the points; the coefficients of these regressions are listed in Table 3. The Pearson product-moment correlation coefficient, r, is also listed, as well as the probability, P, that a noncorrelated sample of data points will give such a coefficient of correlation; this probability was calculated using formulae given in Bevington (1968). N is the number of data points. The coefficients of correlation were calculated for log W–log D and M_B–log $\langle W \rangle$. (Linear regression fits applied to the linear values, i.e., W versus D and M_B versus $\langle W \rangle$, had more dispersion and smaller coefficients of correlation.)

The relation between log D and log W is not the most striking, and statistical tests are certainly needed to reveal any definite trend. Despite obvious scatter, well-defined areas of exclusion exist in the log D–log W diagram (Fig. 2). There are

TABLE 1

GIANT H II REGIONS IN GALAXIES

GALAXY NAME	MORPHOLOGICAL TYPE	NUMBER OF H II REGIONS	$(m - M)$[a]		
			RH	BGPV	dV79
N598 (M33)	Sc(s) II–III	4	24.76	24.18	24.30[b]
N2366	SBm IV–V	3	27.75	26.47	27.10[b]
N2403	Sc(s) III	4	27.78	27.36	27.10[b]
N3938	Sc(s) I	3	31.14	28.74	30.82[c]
N4214	SBm III	1	28.75	25.62	27.47[c]
N4236	SBd IV	3	27.77	26.91	27.70[b]
N4258	Sb(s) II	3	30.38	28.74	...
N4395	Sd III–IV	3	28.76	27.53	...
N4449	Sm IV	4	28.76	27.88	27.86[c]
N4631	Sc(edge)	1	30.43	28.03	27.74[c]
N4656	Im	3	30.43	26.78	...
N5194 (M51)	Sbc(s) I–II	3	30.17	27.60	29.39[c]
N5457 (M101)	Sc(s) I	6	29.47	28.70	28.50[b]
N6822	Im IV–V	3	24.15	25.75	23.73[b]
Ho II	I	1	28.07	26.09	27.7[b]
I2574	S	2	27.77	26.40	27.7[b]

[a] True distance moduli.
[b] de Vaucouleurs 1979*a*.
[c] de Vaucouleurs 1979*b*.

TABLE 2

PHYSICAL PARAMETERS OF GIANT H II REGIONS

H II REGION	TEMPERATURE (K)	ANGULAR DIAMETER[a]	LINEAR DIAMETER (pc) (RH)	(BGPV)	(dV79)	VELOCITY WIDTH (km s^{-1})
N588	10000	31	130	100	110	21.1 ± 1.0
N592	8500[b]	15[c]	65	50	53	17.1 ± 1.0
N595	7350	64	280	210	230	27.1 ± 1.6
N604	9100	81	350	270	280	23.1 ± 0.8
N2366 I	15600	30	520	290	380	22.9 ± 0.6
N2366 II	10000[d]	15.8	271	150	201	23.3 ± 1.0
N2366 III	10000[d]	14.3	246	136	182	19.4 ± 1.2
N2403 I	10000[d]	28.6	500	410	365	29.4 ± 1.1
N2403 II	10000[d]	25.9	452	371	330	28.8 ± 0.8
N2403 III	10000[d]	25.0	436	358	320	29.8 ± 0.8
N2403 IV	8260[b]	12.5[e]	218	179	160	26.1 ± 1.1
N3938 I	10000[d]	7.0	570	190	500	21.3 ± 1.3
N3938 II	10000[d]	5.9	490	160	420	31.3 ± 1.7
N3938 III	10000[d]	7.5	620	200	530	22.7 ± 2.5
N4214 I	10600	20.6	561	132	311	21.1 ± 0.8
N4236 I	10000[d]	12.1	210	141	203	21.9 ± 1.1
N4236 II	10000[d]	13.3	230	155	224	20.5 ± 1.1
N4236 III	10000[d]	17.7	307	206	298	34.2 ± 2.0
N4258 NE	10000[d]	8.0[f]	460	220	...	27.8 ± 1.5
N4258 III	10000[d]	8.0[e]	460	220	...	20.6 ± 1.2
N4258 VI	10000[d]	14.0[e]	810	380	...	34.3 ± 1.6
N4395 I	11970	20.6	564	320	...	23.9 ± 0.8
N4395 II	7750[b]	12.9	353	200	...	28.1 ± 1.9
N4395 III	14450	15.6	427	242	...	33.3 ± 1.8
N4449cm12 + 16	10000[d]	20[e]	550	370	360	32.9 ± 1.1
N4449cm25	10000[d]	18[e]	490	330	330	22.2 ± 0.8
N4449cm22	8975[b]	16[e]	440	290	290	35.8 ± 1.1
N4449cm28	10000[d]	19[e]	520	350	340	20.0 ± 1.0
N4631cm67	10000[d]	17.5[e]	1030	340	...	41.7 ± 2.0
N4656 I	10000[d]	30[e]	1800	330	...	36.3 ± 1.2
N4656 III	10000[d]	14[e]	830	150	...	28.4 ± 1.5
N4656 IV	10000[d]	14[e]	830	150	...	24.7 ± 1.8
N5194cm78	10000[d]	6[e]	310	100	220	29.8 ± 1.3
N5194 I	10000[d]	15.9	833	255	584	35.6 ± 1.8
N5194 III	10000[d]	13.8	723	221	507	34.4 ± 1.4
N5447	9550	23.2[g]	880	617	564	30.0 ± 1.2
N5455	9700	19.3	732	513	469	31.6 ± 1.0
N5461	8800	22.6[g]	857	601	550	35.0 ± 1.3
N5471	14000	25.9	983	689	630	30.2 ± 1.0
Searle 2	7000[b]	11.9[h]	451	316	290	30.3 ± 1.6
Searle 4	7000[b]	11.9[h]	451	316	290	16.9 ± 3.0
N6822 I	11500	49	160	330	130	13.4 ± 0.8
N6822 II	7070[b]	59	190	400	160	19.1 ± 1.9
N6822 III	11000	38	130	260	100	14.7 ± 0.9
Ho II I	10000[d]	22.7	452	181	382	22.0 ± 2.0
I2574 I	13500	18.9	327	175	318	33.2 ± 1.4
I2574 II	10000[d]	13.4	232	124	225	18.0 ± 1.0

[a] Angular diameters are isophotal diameters from Kennicutt 1978 unless otherwise indicated; all angular diameters are in arcsec.

[b] Temperature deduced from the excitation parameter (see text).

[c] Eye estimate (Boulesteix *et al.* 1974).

[d] Canonical value of 10,000 K.

[e] Optical angular diameter (Israel 1980).

[f] Identification uncertain.

[g] Radio continuum angular diameter (Israel, Goss, and Allen 1975, their Tables 2 and 4).

[h] Radio continuum angular diameter (Israel, Goss, and Allen 1975, their Table 9). Radio diameters tend to differ from the optical ones.

no very large H II regions with small velocity width, nor are there small H II regions with large velocity width. From the statistical results of Table 3, a correlation does exist between diameter and velocity width; with the RH distances, this correlation is high ($r = 0.65$) and the very low probability ($P < 10^{-6}$) of zero correlation (that is, of fitting a straight horizontal line through the points) allows one to imply a physical relationship between linear size and velocity dispersion in giant H II regions. The strongest relation, obtained by using RH distances, gives a linear regression of the following form:

$$\log D(\mathrm{RH}) = (1.56 \pm 0.27) \log W + (0.43 \pm 0.39) , \quad (1)$$

where D is the diameter of the H II region in parsecs and W is the e-folding width of the Gaussian Doppler profile, or velocity width in km s^{-1}. Parameters of the linear regression for the distances of BGPV and dV79*a*, *b* are also listed in Table 3.

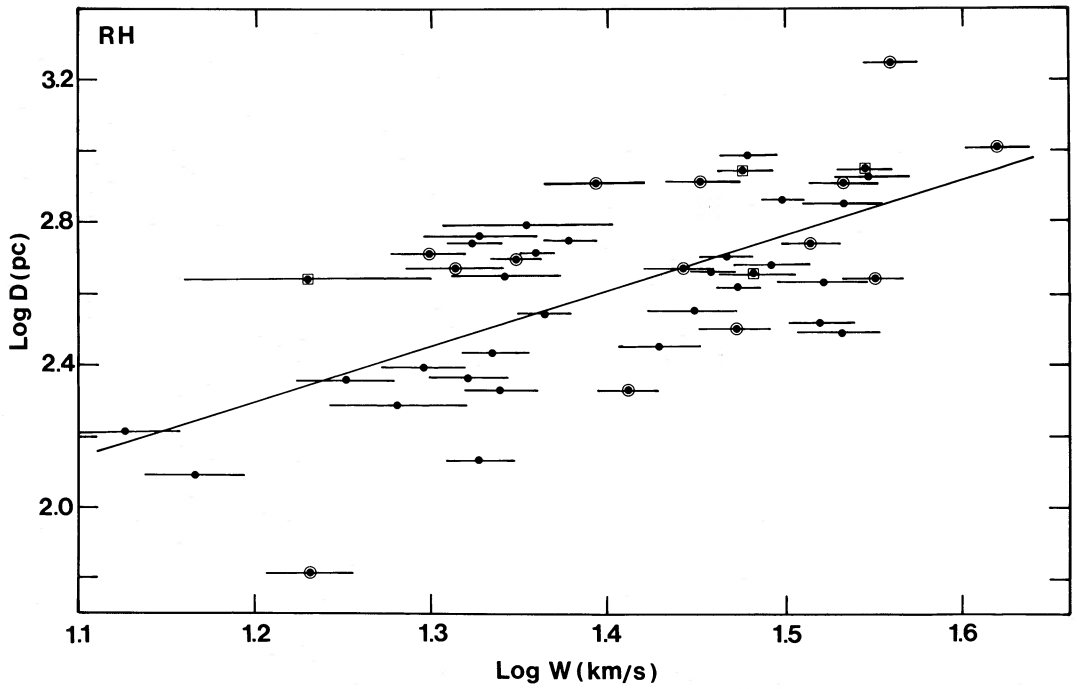

FIG. 2.—Logarithm of the velocity width (log W) of the Hα line profile as a function of the logarithm of the linear diameter (log D) for 47 giant extragalactic H II regions. Linear diameters were calculated from distance moduli deduced from Richter and Huchtmeier (1984). The straight line is the best-fitted linear regression. Uncertainties in the velocity width are listed in Table 2. Dots in circles correspond to data points for which the diameters are from eye measurements; dots in squares are data points where diameters are from radio measurements. All other data points correspond to isophotal diameters measured by Kennicutt (1978).

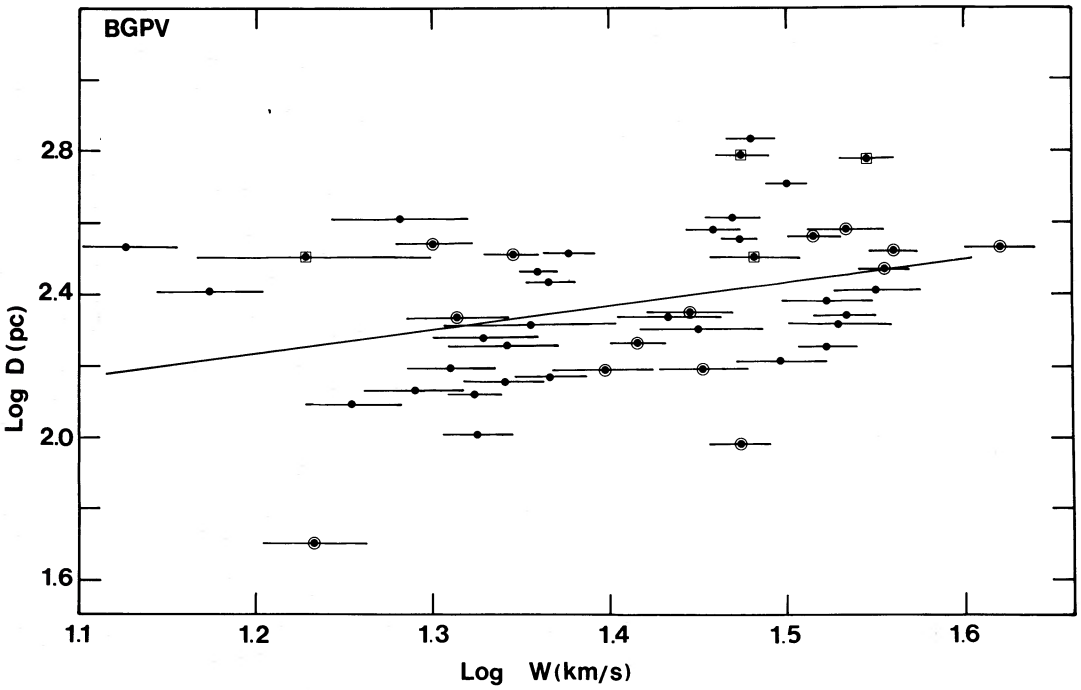

FIG. 3.—Same as Fig. 2, but with linear diameters of giant H II regions calculated from the distance moduli of Bottinelli *et al.* (1984)

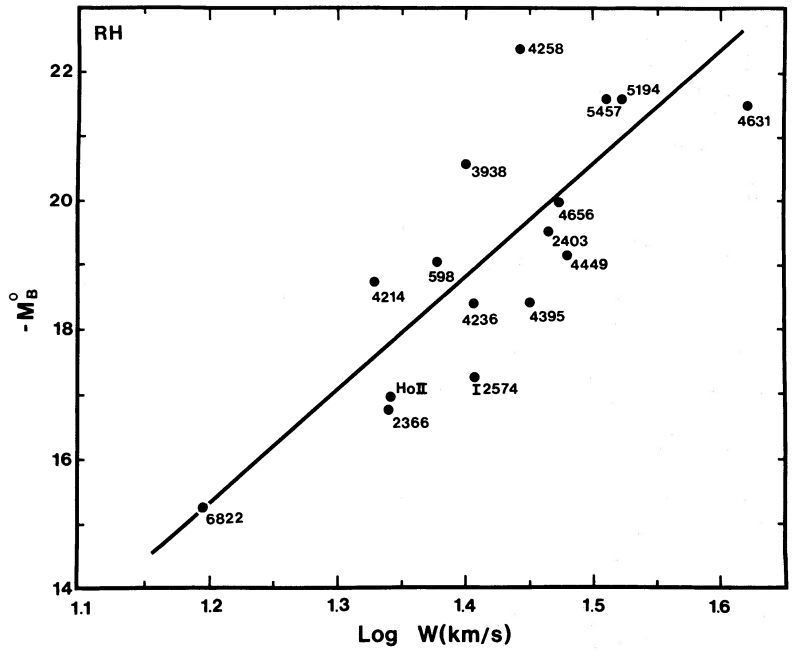

FIG. 4.—Correlation between the corrected absolute blue magnitude of the galaxy M_B after Richter and Huchtmeier (1984) as a function of the logarithm of the mean velocity width (log $\langle W \rangle$) for the H II regions with the largest velocity width in each galaxy as in Table 4.

With BGPV data, any relationship is dubious (Fig. 3). The 37 H II regions with distances from dV79*a*, *b* give also a significant relationship.

When compared with the relation found by Terlevich and Melnick (1981) for a smaller sample of H II regions, equation (1) represents a relation having a smaller power index by 0.25. Using the relationship, obtained with distances of dV79*a*, *b* to 12 galaxies of the sample, leads to a relation with a power index smaller by 0.50 as compared with Terlevich and Melnick. If we use only objects in common with Terlevich and Melnick, we find a relation roughly similar to equation (1). Therefore, the differing slope of equation (1) results only in part from our much larger sample of H II regions; more critical are the use of different angular diameters and distances for the H II regions. These intervening factors probably explain in good part why Gallagher and Hunter (1983) failed to reproduce Terlevich and Melnick's finding and why our data points are much more scattered in the (log D, log W)-plane than those presented in Melnick (1977) and Terlevich and Melnick (1981). Taking into account a precise function for thermal broadening has no important impact using the present data. Uncertainties in distances and in the angular diameters of H II regions remain the dominant sources of error. If we separate the 29 H II regions for which we have isophotal diameters (Kennicutt 1978) from

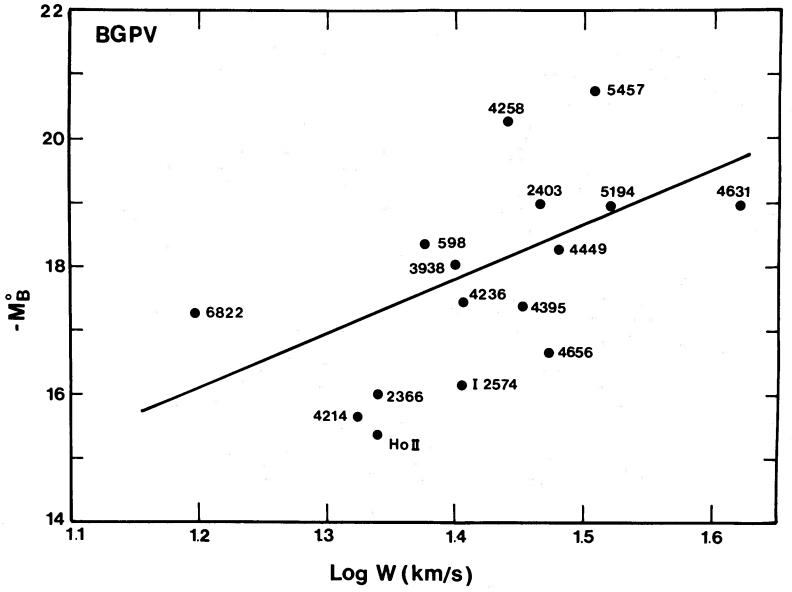

FIG. 5.—Same as Fig. 4, but with absolute magnitude M_B from Bottinelli *et al.* (1984)

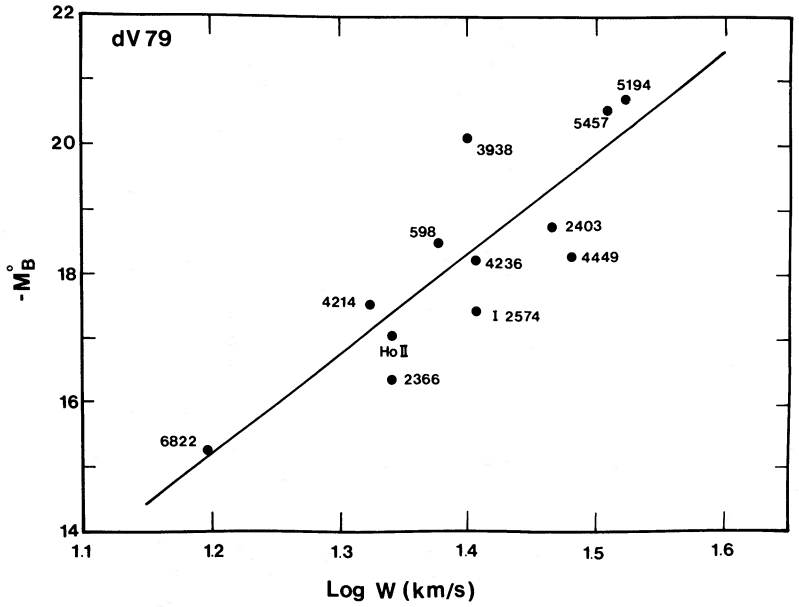

FIG. 6.—Same as Fig. 4, but with absolute magnitude M_B from de Vaucouleurs (1979*a*, *b*)

the remaining 18 where angular diameters were eye measurements, one finds a difference in the correlations. For the H II regions with isophotal measurements, log D is more strongly correlated with log W ($r = 0.72$; $P = 3.4 \times 10^{-5}$) than for the eye measurements ($r = 0.55$; $P = 8.7 \times 10^{-3}$). The uncertainties of the angular diameters of H II regions certainly increase the scatter of the data.

The correlation is much stronger wherever we use the values of RH rather than those of BGPV. This is emphasized when we compare the log $L_{H\alpha}$–log W relations for both sets of distances. Because the Hα luminosity should scale approximately as the square of the diameter of the H II region, the log L–log W relation provides a rough consistency check. For RH distances, a tight correlation ($r = 0.95$) is found between the Hα luminosity and the diameter of the 26 H II regions for which we used the Hα photometry by Kennicutt (1978). The Hα luminosity of H II regions is related ($r = 0.61$; $P < 0.001$) to their velocity width as follows:

$$\text{Log } L_{H\alpha}(\text{RH}) = (3.15 \pm 0.83) \text{ Log } W + (34.9 \pm 1.17) , \quad (2)$$

where $L_{H\alpha}$ is in ergs s^{-1} and W in km s^{-1}. On the other hand, when one uses the BGPV distances for the same subset, the correlation is so weak that we could conclude that it is nonexistent (Table 3). The reason why the BGPV does so poorly can only be that the internal consistency in the distances is particularly poor when this subset of galaxies is considered, and that on average RH distances are inherently more consistent for the 16 galaxies of Table 1.

Because of the known relation between the mean linear diameter of the largest H II regions and the absolute magnitude of a galaxy (Sersic 1960; Sandage and Tammann 1974; Teerikorpi 1985), it is natural to investigate the relationship between M_B and log W. For this purpose, we have taken the mean, $\langle W \rangle$, of the three largest velocity widths in each galaxy (Table 4); because a few galaxies had only one or two H II regions observed, the statistical parameters listed in Table 3 correspond to regressions and correlation coefficients weighted by the number of H II regions in each galaxy (Table 1). Results shown in Table 3 confirm a strong correlation ($r = 0.8$; $P < 0.001$) and a high significance level between M_B and log $\langle W \rangle$. Again, if we consider only the complete samples of RH and BGPV, the correlation is much stronger for the distance moduli of RH. The relation found using RH values of absolute magnitude is

$$M_B(\text{RH}) = -(17.44 \pm 2.21) \log W + (5.55 \pm 3.15) . \quad (3)$$

Our results should be clearly understood. We do not imply that one distance scale is better than the other or that the Hubble constant is more likely to have a certain value rather than another. Our study is restricted to a few nearby galaxies,

TABLE 3

PARAMETERS OF LINEAR REGRESSIONS ($Y = aX + b$)

Y	X	a	b	r	P	N
log D(RH)	log W	1.56 ± 0.27	0.43 ± 0.39	0.65	7.6×10^{-7}	47
log D(BGPV)	log W	0.68 ± 0.28	1.43 ± 0.39	0.34	0.019	47
log D(dV79*a*, *b*)	log W	1.29 ± 0.27	0.65 ± 0.38	0.63	3×10^{-5}	37
log $L_{H\alpha}$(RH)	log W	3.17 ± 0.85	34.90 ± 1.18	0.61	9.4×10^{-4}	26
log $L_{H\alpha}$(BGPV)	log W	0.87 ± 0.99	37.73 ± 1.37	0.18	0.39	26
M_B(RH)	log $\langle W \rangle$	-17.44 ± 2.21	5.55 ± 3.15	0.78	3.7×10^{-4}	16
M_B(BGPV)	log $\langle W \rangle$	-8.43 ± 2.26	-6.01 ± 3.22	0.51	0.044	16
M_B(dV79)	log $\langle W \rangle$	-15.48 ± 1.81	3.38 ± 2.55	0.85	4.7×10^{-4}	12

TABLE 4

ABSOLUTE MAGNITUDE OF GALAXIES (corrected) AND MEAN VELOCITY DISPERSION OF H II REGIONS

GALAXY	$-M_B$ RH	$-M_B$ BGPV	$-M_B$ dV79	log $\langle W \rangle$
N598	19.07	18.38	18.50[a]	1.377
N2366	16.72	16.00	16.37[a]	1.340
N2403	19.49	19.01	18.75[a]	1.467
N3938	20.54	18.07	20.15[b]	1.400
N4214	18.72	15.69	17.54[b]	1.324
N4236	18.42	17.45	18.24[a]	1.407
N4258	22.34	20.29	...	1.441
N4395	18.41	17.39	...	1.453
N4449	19.11	18.28	18.26[b]	1.481
N4631	21.45	18.94	...	1.620[c]
N4656	19.98	16.66	...	1.474
N5194	21.60	18.93	20.72[b]	1.522
N5457	21.58	20.78	20.58[a]	1.509
N6822	15.25	17.26	15.24[a]	1.196
Ho II	16.93	15.37	17.04[a]	1.342[c]
I2574	17.27	16.14	17.44[a]	1.408[d]

[a] From primary and secondary indicators (cf. de Vaucouleurs 1978, 1979*a*).

[b] From tertiary indicators (cf. de Vaucouleurs 1979*b*).

[c] One H II region observed.

[d] Two H II regions observed.

and it is only for this set of galaxies that we can make a comparison. While RH distances to the 16 galaxies of our sample appear to be more consistent than those of BGPV, the overall distance scale inferred by BGPV might well be closer to reality. Our study does not and cannot imply any conclusion on the global merits of each distance scale. However, it should be noticed that BGPV distance moduli and absolute magnitudes (Tables 1 and 4) are clearly at odds with those of dV79*a*, *b* for several galaxies.

Distances as determined by RH are consistant with the Sandage and Tammann methodology. (Distance moduli and absolute magnitudes taken from Sandage and Tammann 1981 would have given essentially the same results.) One might therefore argue that it is only natural that the log *D*–log *W* and M_B–log $\langle W \rangle$ relationships are stronger with RH distances, because Sandage and Tammann have given large weight to H II region diameters as a distance indicator. The relations found would therefore be circular in their meaning. This argument flounders on two points: First, as shown in RH, diameters of H II regions were not the main distance indicators for the nearby galaxies of our sample; stellar indicators were used in a majority of cases. Second, the log *W*–log *D* and M_B–log $\langle W \rangle$ relationships resist surprisingly well the vagaries of different distance scales. For example, true distance moduli and absolute magnitudes from dV79*a*, *b* for 12 galaxies of our sample (Tables 1 and 4) produce significant relationships (Table 3). The relationship is even stronger for M_B–log $\langle W \rangle$, where dV79*a*, *b* gives more significant results than RH. For the 12 galaxies of dV79*a*, *b*, the relationship ($r = 0.85$; $P < 0.001$)

$$M_B(\text{dV79}) = -(15.48 \pm 1.81) \log W \pm (3.38 + 2.55) \quad (4)$$

is fairly close to the calibration of velocity dispersion as a distance indicator proposed by de Vaucouleurs (1979*c*). The main point is that the relationships survive the different distance scales and take slightly different forms depending on the adopted distances to the galaxies. (Compare Figs. 4 and 6.) The reader should be aware, however, that the numerical values in equations (3) and (4) are only indicative of a trend, and they should be used with the greatest caution in any application.

To summarize: We believe that, in spite of the poor results obtained with the distance parameters of BGPV, the correlation log *D*–log *W* has a high statistical significance. We deduce that the distances of BGPV to the 16 galaxies of our sample are less consistent than those of RH. The slope of the relationship implied by our observations (Table 3) is significantly less than that found by Melnick (1977) and Terlevich and Melnick (1981). A strong correlation is found between the absolute blue magnitude of the parent galaxy and the mean of the three largest velocity dispersions of its H II regions. Distance parameters from de Vaucouleurs (1978; 1979*a*, *b*) provide the strongest correlation between M_B and log $\langle W \rangle$.

VI. DISCUSSION

To evaluate the mechanisms explaining the relationships between the velocity width of the Hα profile and the size of giant H II regions, some features of these objects should be brought to attention. Because their spectra can be ordered with a single parameter which is the line ratio ([O II] + [O III])/Hβ, giant H II regions are considered photon bounded (McCall, Rybski, and Shields 1985). Their average rms density is as low as 1–10 cm^{-3} (Kennicutt 1984), a density close to that of the intercloud medium. What appears as a single H II region often turns out to be an aggregate of multiple H II regions, when observed under excellent seeing conditions; high-resolution echelle spectroscopy reveals a complex velocity structure (Rosa and Solf 1984; Skillman and Balick 1984). Several clusters of stars may be embedded in a single giant H II region (Kennicutt 1984; Hunter and Gallagher 1985; McCall, Rybski, and Shields 1985). Our study indicates that the log *D*–log *W* relation is maintained despite the internal multiple structure of giant H II regions. Multiplicity might explain slight asymmetries in some of the integrated Fabry-Perot line profiles, but the velocity width still relates to the overall size of the complex.

These observations make it very hard for models based on stellar winds or cavities blown by hidden supernovae to explain the observed log *D*–log *W* relationship. Stellar winds or chains of supernova explosions would blow bubbles which could be observed as expanding shells. Such shells lead to the following problems: (1) Expanding shells eventually reach terminal velocities because of gravitational deceleration perpendicular to the plane of the galaxy and because of the ambient density stalling (snowplow) effect (Bruhweiler *et al.* 1980). Consequently, the largest velocities ought to be expected at the smallest scales; for example, planetary nebulae show a decrease of expansion velocity at the larger sizes (Sabbadin, Ortolani, and Bianchini 1985). (2) Models based on stellar wind bubbles can explain in part the internal velocity fields of individual giant H II regions, but fail to make predictions of the global relationships log *D*–log *W* and M_B–log $\langle W \rangle$. (3) because they are very thin compared with their radii, evolved shells appear as ringlike features. This means that most of the light contributed by these shells comes from the sections moving in the plane of the sky, and are those with the least dispersion in radial velocity. Such geometry makes it very difficult to produce a velocity-size relationship as the observed one.

Champagne flows, caused by hot star formation near the edge of a giant molecular cloud, are likely to exist in giant H II complexes. The model (Tenorio-Tagle 1979; Bodenheimer, Tenorio-Tagle, and Yorke 1979) predicts large supersonic velocities, the amplitude of which is dependent on the ratio

of the density of the molecular cloud with respect to that of the intercloud medium. Multiple champagne flows are probably prevalent, but again it is not clear how they can produce the observed scaling of velocity with size. The model predicts terminal velocities; these velocities are probably reached relatively close (compared with the overall size of giant H II regions) to the molecular cloud which is giving birth to OB stars. Like stellar wind–blown bubbles, champagne flows may be restricted to the inner regions relatively close to the molecular clouds; these regions could correspond to the "nuclei" identified by Skillman and Balick (1984). As in the case of bubbles, the ram pressure of champagne flow reaches equilibrium with the pressure of the diffuse galactic medium which eventually contains them at some stage. Again, no direct explanation of the M_B–log $\langle W \rangle$ relationship is provided.

Two mechanisms avoid the problems of geometry and of stalling at very large scales; they are gravitation and turbulence. Self-gravitation of the star and gas complex forming giant H II regions was actually proposed by Terlevich and Melnick (1981) as responsible for the relationship between velocity dispersion and size. This was based on the $D \propto V^2$ relationship inferred from their observations; virialized motion in a system in pressure equilibrium obeys a $V \propto D^{1/2}$ law. However, our results (eq. [1] and Table 3) lead to relationships with a power index smaller by 0.45 (RH) or by 0.7 (dV79*a*, *b*) than the value predicted by the virial equilibrium. Consequently, our results are inconsistent with self-gravitation. Several workers (Gallagher and Hunter 1983; Rosa and Solf 1984; Skillman and Balick 1984; Hippelein and Fried 1984) have already questioned the importance of gravitation in the dynamics of H II regions, the general impression being that, apart from exceptionally large H II complexes such as NGC 5471 in M101 and isolated H II regions (blue compact galaxies), total mass is unlikely to be sufficient for gravitation to play a dominant role. Gravitation may play a role in some giant H II regions, but gasdynamical processes determine the gas kinematics in most instances in H II complexes.

a) Turbulence in H II *Regions*

To explain the scaling of velocity dispersion with size, we propose that a fundamental hydrodynamic process, turbulence, is at play. Several theoretical considerations indicate that the interstellar medium is likely to be turbulent (von Weizsäcker 1951; Kaplan 1966; Kaplan and Pikel'ner 1970). This results from the observation that the linear scale of fluctuations of most physical properties is much larger than the mean free path in a neutral medium and than the Coulomb mean free path in ionized regions; inertial forces dominate over viscous stresses, and transport properties are described by the bulk motions of the gas. Turbulence extracts energy from the mean flow at large scales, and this gain is approximately balanced by viscous dissipation at very small scales (Tennekes and Lumley 1972). Dimensional analysis and the Kolmogorov similarity hypothesis are used to measure the energy dissipated in a turbulent cascade in an incompressible fluid (von Weizsäcker 1951; Kaplan 1966). Energy is transferred from the largest eddies to the smallest ones at a constant rate. The specific turbulent luminosity, S, in a hierarchy of eddies in a turbulent cascade is given by

$$S = \eta(\nabla \times V)^2 , \tag{5}$$

where $\eta = \rho L V$ is the momentum carried by the turbulence; ρ is the density and L is the linear scale under consideration. The term $(\nabla \times V)$ can be approximated as V/L. Assuming steady state and using similarity arguments, it can be shown that the turbulent energy flow is constant at all vortex sizes, which means that S is independent of the scale L (von Weizsäcker 1951). In other words,

$$s = \rho v^3 / L = \text{constant} . \tag{6}$$

This relation, which is Kolmogorov's law (Kolmogorov 1941), predicts that, in a turbulent flow, the relative velocities between two points separated by a distance L will scale as $L^{1/3}$. This assumes that the density in the medium does not vary much over the nebula; if one compares H II regions with different mean densities, one should take into account equation (6) (Fleck 1983). Moreover, the Mach number in H II regions is often larger than unity, making the medium compressible; further dissipation through shock waves can also be present. These effects should combine to make the V-L relation steeper than the one predicted by Kolmogorov (Fleck 1983; Roy and Joncas 1985). Turbulence should apply at all nebular scales and hold despite the multiple structure of giant H II complexes, simply because these aggregates behave as different eddies linked together through the same energy cascade.

One fundamental characteristic is the irregularity, or randomness, of all turbulent flows, which forces us to rely on statistical methods to study them (Tennekes and Lumley 1972). Statistical methods (Kaplan 1966; Kaplan and Pikel'ner 1970; Scalo 1984), based on the search for a correlation between velocity fluctuations and the projected distance between the velocity points, are the best suited to investigate the presence of turbulence in H II regions. Several years ago, von Hoerner (1951), Courtès (1955) and Münch (1958) searched, with marginally encouraging results, for this correlation from radial velocity measurements in the Orion Nebula. The method was also applied to a detailed radial velocity map of a molecular cloud by Scalo (1984). Roy and Joncas (1985) have successfully applied the method to detailed velocity maps of two galactic H II regions (see the Appendix). Because it computes a point-to-point correlation, the structure function is a direct method for establishing how velocity fluctuations vary as a function of linear separation. The main problem, in its astronomical application, remains projection smearing; separations between points are measured as projected on the plane of the sky. However, Scalo (1984) has shown that projection effects will significantly affect the shape of the structure function only at scales much smaller than the diameter of the object. The Appendix summarizes the application of the structure function to the radial velocity maps of two galactic H II regions (M17 and S142).

Unfortunately, from the points of view of telescope time and data reduction effort, it is an almost impossible task to obtain the extensive radial velocity maps needed to calculate the structure function for many H II regions. Furthermore, many objects, such as extragalactic H II regions, are too small in angular size to make the exercise fruitful; several hundreds of velocity point pairs are needed to calculate a significant structure function. An alternative technique for searching for turbulence in the interstellar medium has been to deduce the internal velocity dispersion from the velocity width of integrated spectral line profiles. If the gas motions in a nebula have a Maxwellian distribution, the e-folding width of the Gaussian line profile corresponds to the most probable velocity in the nebula

(Smith and Weedman 1970). One can therefore see whether this velocity width is related to the sizes of nebulae.

Extracting information about velocity fluctuations from line widths is subject to some pitfalls (Scalo 1984). Nevertheless, several studies on the dynamics of molecular clouds have used this approach (Larson 1979, 1981; Leung, Kutner and Mead 1982; Myers 1983; Henriksen and Turner 1984; Stenholm 1984); there is some controversy about the exact shape of the relation, but the CO velocity widths β appear to scale with the diameters D of molecular clouds as $\beta \propto D^{1/5}$ (Fleck 1983). Because of the aperture dilution effect discussed later, this relation and its spectral index do not have the same exact physical meaning as the ones deduced from the structure function, but they are related. Furthermore, it is not clear whether molecular clouds are supported by turbulence; it is also possible that one observes the tendency of molecular clouds to reach virial equilibrium (Fleck 1983).

For H II regions, one expects gravitation to have only a minimal influence compared with the hydrodynamical processes. Applying standard linear regression analysis techniques to our data on giant extragalactic H II regions, we calculated the relation between log W and log D, where the velocity widths of giant extragalactic H II regions (Table 2) now correspond to the dependent variable and the diameters to the independent variable. Using the diameters of giant extragalactic H II regions as given by the RH distances to the parent galaxies, a linear regression fit leads to a power law of the form

$$W = (5.0 \pm 1.3)D^{0.27 \pm 0.05} . \quad (7)$$

The observed relation is shown in Figure 7 labeled as *GEHR*. When distances from de Vaucouleurs (1978, 1979*a*, *b*) are used for a subset of 35 giant H II regions, the relationship is

$$W = (4.4 \pm 1.4)D^{0.31 \pm 0.06} . \quad (8)$$

One cannot simply invert equation (1) to obtain W as a function of D. Because the coefficient of correlation is not equal to unity, one must calculate a new linear regression minimizing the dispersion of log W versus log D.

b) Scaling of Velocity Dispersion as a Function of Linear Size in H II *Regions*

In order to be able to compare the result of equation (7) with that which would be given by the structure function if it could be calculated, we have analyzed the velocity fields of the galactic H II regions S142 and M17, for which we could calculate the structure functions (see Appendix). We established the internal relationship between velocity width and linear size. This was achieved by numerically simulating a Fabry-Perot spectrometer which would sample the nebulae with diaphragms of varying size. This was done by gridding our extensive velocity maps of S142 and M17, and by measuring the dispersion from

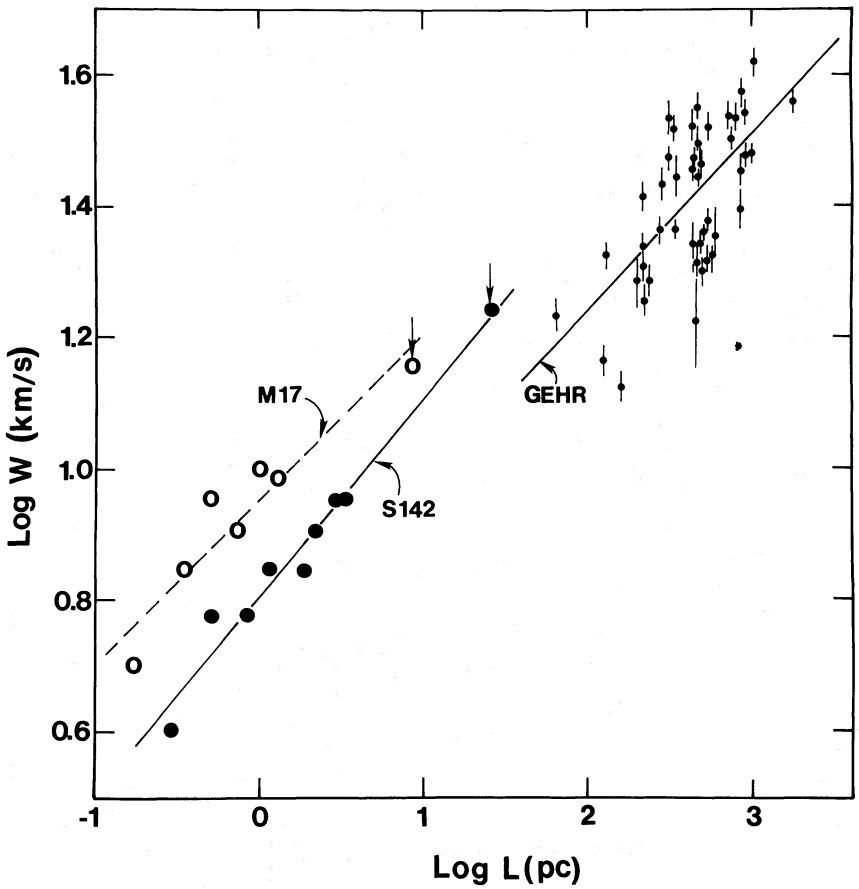

FIG. 7.—Velocity dispersion as a function of linear size in the two galactic H II regions M17 and S142, and in 47 giant extragalactic H II regions. The lines are linear regressions fitted to the different sets of data points. These regressions can be represented by a power law of the form $W = AL^n$, where $n \approx 0.3$, and where A is different for each set of data.

the mean velocity for every window where 11 or more radial velocities had been measured. Successive grids with window size ranging from 15″ to 180″ were used; these mesh sizes were chosen, first, to ensure a sufficent number of windows with a large number of measured velocities within each one and, second, to be small enough to avoid the effect of large-scale velocity gradients which become obvious on scales of several minutes of arc. For each grid, we produced an histogram of the velocity dispersion measured in each window (Roy and Joncas 1985). Then we used the most probable dispersion velocity given by each histogram as the characteristic velocity width of the corresponding window size. Figure 7 shows, for S142 and M17, log W, where W is the velocity width given by this most probable dispersion velocity, as a function of log L, where L is the corresponding mesh size in parsecs. Added to this figure are the e-folding widths (points shown with an arrow in Fig. 7) of the velocity histograms of S142 and M17. Best-fitted linear regressions are also shown and correspond to the following power laws:

$$W(\mathrm{S142}) = (6.4 \pm 1.0)L^{0.31 \pm 0.02}, \quad (9)$$

$$W(\mathrm{M17}) = (9.0 \pm 1.0)L^{0.25 \pm 0.04}. \quad (10)$$

The relations have the same slopes within the errors. The difference in their Y-intercept (A) could be explained in part by the uncertainty in their distance. However, in a turbulent energy cascade, the constant A corresponds to the cubic root of the specific dissipation rate ($\mathrm{m^2\ s^{-3}}$) and equivalently to the supply rate, indicating that more kinematic energy might be supplied to eddies in M17 than in S142. Moreover, the relations log W–log L for S142 and M17 roughly have, within errors, the same slope (~ 0.3) as that established from the line widths of giant extragalactic H II regions (see eqs. [7] and [8] and Fig. 7).

It is not clear whether this coincidence of slopes is fortuitous. Despite the nature of turbulence which predicts a similar spectrum within and among objects of similar nature (Henriksen and Turner 1984), one should be cautious in comparing the slopes of M17 and S142 with the slope produced by the 47 individual giant H II regions. The constant A, scaling the velocity dispersion with respect to size, is smaller in giant extragalactic H II regions. It is unlikely that the difference is due to distance uncertainty only. Such distance discrepancies would imply that the diameters of extragalactic H II regions, hence distances of the parent galaxies, are overestimated by a factor of 3; although the diameters of the extragalactic H II regions were established with distances from Richter and Huchtmeier (1984) which are consistent with the Sandage-Tammann distance scale, the consistency between equations (7) and (8) suggests this bold explanation to be unnecessary. Instead it appears that, for the same characteristic nebular size, a galactic H II region has a larger velocity dispersion than its extragalactic counterpart.

The results obtained from the calculation of the structure function in S142 and in M17 show that there is a correlation which corresponds to a scaling of $\Delta V \propto L^{1/2}$ for a limited range of scales (see Appendix). The steeper slope compared with the predicted one, $n = \frac{1}{2}$ instead of $n = \frac{1}{3}$, is not unexpected because the Kolmogorov law applies strictly to subsonic ($v < V_{\mathrm{th}}$) and incompressible fluid flows. In an H II region $v > V_{\mathrm{th}}$, and the medium must be treated as compressible; moreover, velocity fluctuations are supersonic for scales $r > 1$ pc. The main effect of compressibility (for $\delta\rho/\rho \ll 1$) is that the gas loses energy in the form of sound waves which dissipate into heat (Lighthill 1955). For large ratios of $\delta\rho/\rho$, shocks could become the major dissipation mechanism. With energy dissipation amplified either way, less turbulent energy is left for the smaller eddies of the turbulent cascade. If turbulence is present, its energy cascade will display a steeper slope than predicted (Roy and Joncas 1985; Fleck 1983). This is what we observe in S142 and M17.

Why does the method using the velocity widths of line profiles give a relation log W–log L which is less steep than the one implied by the structure function for the same object? This is merely due to the fact that sampling by a diaphragm (real as in a Fabry-Perot spectrometer, or numerical as in the gridding of a velocity map) produces a mean of *all* velocities measured *within* the diaphragm, hence diluting all scales smaller than the diaphragm size. This diminishes the effective dispersion velocity of the larger sizes relative to the small sizes. The number of velocity points (or scales) increases roughly as the square of the diaphragm diameter or size; consequently, the larger scales are more heavily weighted by the velocity dispersions characteristic of small scales. This results in a less steep relation between log W and log L than the one given by the structure function. If the rough ratio between the relationships ΔV-L obtained from the structure function and the relationship W-L given by the line-width method can be extrapolated to giant extragalactic H II regions, it means that $\Delta V \propto L^{1/2}$ for nebular scales ranging from 1 to 1000 pc.

c) *Origin of Turbulence in Giant* H II *Regions*

Turbulence means energy transfer from large eddies to smaller ones until it dissipates into heat at scales where viscosity smooths out the velocity fluctuations. Continuous energy supply is needed for the cascade not to die with the vanishing, first, of the smallest cells because the characteristic time for dissipation (or formation) of eddies is proportional to $L^{2/3}$ (von Weizsäcker 1951). As we have suggested (Roy and Joncas 1985), Kelvin-Helmholtz (K-H) instabilities are likely to arise in the forming and bursting of H II regions out of molecular clouds. The pressure gradient, maintained by the photoionizing stellar flux as long as there is neutral material to ionize, will drive a flow of high-speed gas into the intercloud medium (Bodenheimer, Tenorio-Tagle, and Yorke 1979). The sheared interface will give rise to K-H waves which will convect to the origin of the flow along the interface, and transversely into the nebula, making it completely turbulent in 10^5–10^6 years (Blake 1972; Roy and Joncas 1985). Giant extragalctic H II regions are much larger, and velocity shears could be induced at large scales by a firework of champagne flows (Tenorio-Tagle 1979) bursting out all around the periphery of a giant molecular cloud.

One other possibility suggested long ago by von Weizsäcker (1951) and more recently by Fleck (1981) is to use the transverse velocity shear resulting from the differential rotation of a galaxy to produce the largest eddies. There is observational support for tapping the rotational energy reservoir in the relationship observed between the absolute magnitude (related to rotation via the Tully-Fisher relation) and the mean velocity width of the line profiles of the largest H II regions in a galaxy. Fleck (1981) has shown that velocity shears of the order of twice the Oort constant A can be generated; in a galaxy such as ours, this amounts to 30–50 $\mathrm{km\ s^{-1}\ kpc^{-1}}$. Giant molecular clouds, star clusters, and H II regions with their champagne flows are born within the largest eddies. We suggest that the

UV photon flux produced by several clusters of early-type stars is not bound by the gas of the champagne flow, but penetrates beyond to ionize a large volume of diffuse galaxian gas. This gigantic fluorescent volume of ionized material appears to us as a giant H II region, and its large-scale velocity field is dominated by galaxian turbulence. Most of the giant H II regions would be made up of these huge tenuous ionized balloons of gas. It is known that the luminosity of the brightest blue supergiants increases with M_B for parent galaxies brighter than $M_B = -17$ (Sandage and Tammann 1982). It is likely that more luminous galaxies have clusters richer in those luminous supergiants. These more luminous UV powerhouses ionize larger volumes of interstellar gas, unveiling larger eddies of the turbulent galaxian velocity field. The strength of shear in the differential rotation and therefore the amplitude of the velocity fluctuations in the turbulent flow depend on the velocity of rotation of the galaxy. Since the latter depends on the total galaxian mass, it tightens the relationship between M_B and $\log \langle W \rangle$ for giant H II regions; turbulent stirring is more powerful in more luminous galaxies because they have more mass. We have a simple, direct explanation for the relationship between M_B and $\log \langle W \rangle$.

However, several giant H II regions observed in irregular systems, known to be weak rotators, also display large velocity dispersions. Although turbulence is a promising mechanism for understanding the W-L relation, some points need to be clarified: can other dynamical morphologies produce a power-law correlation over a large range of nebular scales? What drives the largest eddies in giant H II regions? Is the mismatch in the W-L relationships at galactic and extragalactic scales due to a distance problem? Maps of the neutral hydrogen velocity field obtained with high spatial resolution should show a similar scaling of velocity fluctuations as a function of linear sizes; such observations would provide a crucial test of the existence of turbulence already present in the galaxian velocity field.

VII. SUMMARY

The main results of our study of integrated Hα line profiles of a large number of giant extragalactic H II regions are the following:

1. The velocity width, W, of the Hα line profiles measured in 47 giant H II regions belonging to 16 late-type spirals and Magellanic irregulars is found to be related to the size of the H II region. The relationship found is $W \propto D^n$, where $n < 1.6$; this is significantly different from the prediction of self-gravitation.

2. The mean of the three largest velocity widths of H II regions in a galaxy is closely related to the absolute blue magnitude of the parent galaxy. The strongest correlation is obtained for a restricted sample of 12 galaxies for which de Vaucouleurs (1978; 1979*a*, *b*) derived distance moduli from the use of several primary, secondary, and tertiary indicators.

3. The shape of the relation log D–log W is dependent on the adopted distances to the galaxies. Assuming that a physical relationship exists between velocity dispersion and size, we conclude that the distance moduli established by Richter and Huchtmeier (1984) have a better internal consistency than those of Bottinelli *et al.* (1984); this comment applies only to the sample of 16 nearby galaxies that we observed.

4. Analysis of detailed velocity maps of two galactic H II regions (M17 and S142) shows that the internal relationship between the velocity width, W, and linear size, L, is, within the errors, the same as for giant extragalactic regions, that is, $W \propto L^{0.3}$.

5. A turbulent energy cascade is suggested as the most viable mechanism explaining both the relationship between velocity dispersion and size and that between velocity dispersion and the absolute magnitude of the parent galaxy. The transverse shear due to differential rotation could supply the kinetic energy to the largest cells. Giant H II regions are produced by the unbound UV photon flux which ionizes large volumes of galaxian gas whose velocity field is dominated by already existing turbulence.

We thank R. C. Kennicutt, who provided material and several suggestions at the start of this project. Bernard Malenfant and Réjean Bisson gave enthusiastic technical support. Jeremy R. Walsh, John R. Lucey, and Keith Taylor provided numerous helpful comments. We are grateful to the Canada-France-Hawaii Telescope Corporation staff for their assistance during a most successful observing run on the 3.6 m telescope. One of us (J. R. R.) thanks Donald C. Morton and the Anglo-Australian Observatory staff for their kind hospitality while on research leave from Université Laval. Generous funding was provided by the National Research Council of Canada, the Natural Sciences and Engineering Research Council of Canada, and the Fonds FCAC of the Government of Québec.

APPENDIX

This appendix summarizes the results of the search for correlation between velocity fluctuations and linear size in two galactic H II regions. A Fabry-Perot camera was used to map the velocity fields of M17 and S142. Many thousands of velocity points were measured across the surface of the objects. The observations were obtained with the 1.60 m telescope of the Observatoire astronomique du mont Mégantic. Observational procedures, data on the observed H II regions, and other results have been published elsewhere (S142: see Joncas and Roy 1984*a*, *b*; Roy and Joncas 1985; M17: see Joncas and Roy 1985).

If an H II region is turbulent, fluctuations in density and velocity are present. The mean velocities measured along different lines of sight will exhibit fluctuations in excess of measurement errors. The method of correlation (Kaplan 1966; Kaplan and Pikel'ner 1970) can be used to study these fluctuations. Turbulence implies that such fluctuations will scale as some power of their linear separation. One may use the correlation function $D(r) = v(r')v(r'')$ or the structure function $B(r) = [v(r') - v(r'')]^2$, where $r = r' - r''$ and $v(r')$ and $v(r'')$ are the radial velocities measured at positions r' and r'', and r is the scale investigated for correlation. Specific criteria are to be satisfied for using these functions (Kaplan 1966; Scalo 1984; Roy and Joncas 1985). Scalo (1984) has shown that it is advantageous to use the structure function for the study of interstellar clouds. The observed structure function can then be compared with theoretical models; for example, Kolmogorov law predicts that $\Delta V \propto r^{1/3}$, that is, $B(r) \propto r^{2/3}$. The structure function does not reveal

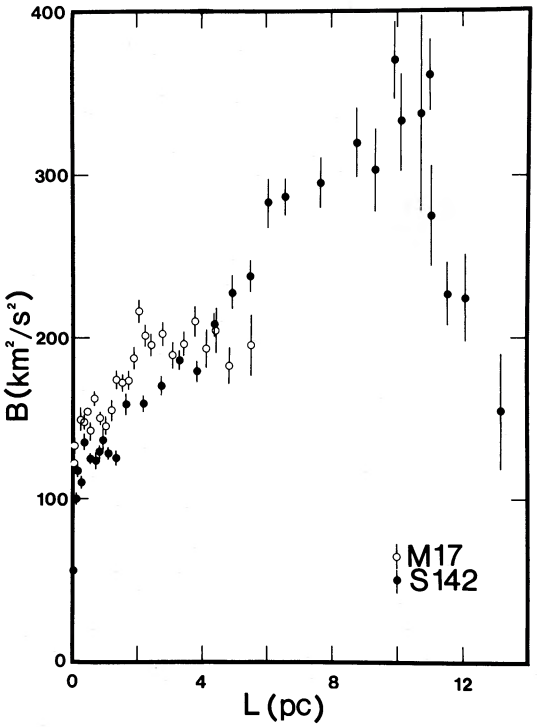

FIG. 8.—Structure function, B, as a function of projected linear separation, L, between radial velocity points. The vertical bars correspond to the statistical uncertainties of the calculated points. Filled circles are the data points for S142, and open circles are those for M17.

the exact characteristic of nebular turbulence, but it produces evidence of statistical order, which is an inherent property of turbulence.

After removing large-scale gradients (cf. Scalo 1984), we have calculated the structure functions for the H II regions M17 and S142. S142 is a large (30 pc diameter), evolved H II region with a low mean density ($n = 25$ cm^{-3}) at a distance of 3.5 kpc, and M17 is a smaller (the central and brightest section has a diameter of 10 pc), denser ($n = 400$ cm^{-3}), and younger region at a distance of 2.2 kpc. The large number of accurate (± 1–2 km s^{-1}) radial velocities measured across these two objects [S142: 40,983 V(lsr); M17: 9054 V(lsr)] allows the calculation of statistically reliable structure functions which are shown in Figure 8. The projected angular separations have been converted into projected linear separation.

Three distinct regimes are observed: (1) for 1.6 pc $< r <$ 9 pc in S142 and $1 < r < 2$ pc in M17, the structure function is well represented by $B(r) \propto r$, which means that $\Delta V \propto L^{1/2}$; this is a steeper slope than expected from the Kolmogorov law. (2) For small values of r, i.e., $r < 1.6$ pc (S142) and $r < 1$ pc (M17), $B(r)$ does not approach zero. This behavior of the structure function at small r is easily explained by projection effects. Indeed, each measured radial velocity fluctuation refers to two points seen in projection on the apparent surface of the nebula; however, the emission may originate from greatly differing depths for two nearby lines of sight. Therefore, one should expect that $B(r)$ corresponding to $r \ll d$, where d can be either the geometrical length corresponding to one optical depth or—more likely—the characteristic distance between the nebular filaments, will be high; indeed, large velocity differences are likely for some of the points separated by $r \ll d$. The observed structure function should show a change of slope or some leveling off below a certain scale; this is best seen in plots of log B against log L, as shown for S142 in Roy and Joncas (1985) and for M17 in Joncas and Roy (1985). It would be interesting to follow the behavior of the structure function for scales $r \ll 1$ pc to see whether $B(r)$ changes at subsonic velocities. But this could be done only by observing more nearby H II regions. (3) For a scale $r > 9$ pc (S142) and $r > 2$ pc (M17), there is decorrelation as if turbulence had not yet had the time to make the whole nebula turbulent. On the other hand, our method may be hampered by large scale gradients in the velocity field which act as "noise" at large scales or to the inadequacy of the spatial correlation approach in dealing with large eddies (Cantwell 1981).

To summarize: (*a*) Correlation between velocity fluctuations ΔV and projected linear separation L is observed for a limited range of linear scales in both S142 and M17; it corresponds to a relation of the form $\Delta V \propto L^{1/2}$. This is consistent with the presence of turbulence. (*b*) At small scales ($L < 1$ pc), the structure function does not approach zero; correlation may exist, but smearing of the three-dimensional fluctuation pattern onto a two-dimensional projection may be too severe. (*c*) At scales corresponding to approximately the radius of the nebulae and larger, there is decorrelation; it is not clear whether this happens because there are no eddies of that size or because of the limits of the correlation method.

REFERENCES

Arsenault, R., and Roy, J.-R. 1984, *Pub. A.S.P.*, **96**, 496.
Bevington, P. R. 1968, *Data Reduction and Error Analysis for the Physical Sciences* (New York: McGraw-Hill), p. 122.
Blake, G. M. 1972, *M.N.R.A.S.*, **156**, 67.
Bodenheimer, P., Tenorio-Tagle, G., and Yorke, H. W. 1979, *Ap. J.*, **23**, 85.
Bottinelli, L., Gougenheim, L., Paturel, G., and de Vaucouleurs, G. 1984, *Astr. Ap. Suppl.*, **56**, 381 (BGPV).
Boulesteix, J., Courtès, G., Laval, A., Monnet, G., and Petit, H. 1974, *Astr. Ap.*, **37**, 33.
Bruhweiler, F. C., Gull, T. R., Kafatos, M., and Sofia, S. 1980, *Ap. J.* (*Letters*), **238**, L27.
Cantwell, B. J. 1981, *Ann. Rev. Fluid Mech.*, **13**, 457.
Courtès, G. 1955, in *IAU Symposium 2, Gas Dynamics of Cosmic Clouds*, ed. H. C. van de Hulst and J. M. Burgers (Amsterdam: North-Holland), p. 131.

de Vaucouleurs, G. 1978, *Ap. J.*, **224**, 710.
———. 1979*a*, *Ap. J.*, **227**, 380 (dV79*a*).
———. 1979*b*, *Ap. J.*, **227**, 729 (dV79*b*).
———. 1979*c*, *Astr. Ap.*, **79**, 274.
Dyson, J. E. 1979, *Astr. Ap.*, **73**, 132.
Fleck, R. C. 1981, *Ap. J. (Letters)*, **246**, L151.
———. 1983, *Ap. J. (Letters)*, **272**, L45.
Flynn, F. H. 1966, *M.N.R.A.S.*, **134**, 53.
Gallagher, J. S., and Hunter, D. A. 1983, *Ap. J.*, **274**, 141.
Henriksen, R. N., and Turner, B. E. 1984, *Ap. J.*, **287**, 200.
Hippelein, H., and Fried, J. W. 1984, *Astr. Ap.*, **141**, 49.
Hunter, D. A., and Gallagher, J. S. 1985, *A.J.*, **90**, 80.
Israel, F. P. 1980, *Astr. Ap.*, **90**, 246.
Israel, F. P., Goss, W. M., and Allen, R. J. 1975, *Astr. Ap.*, **40**, 421.
Joncas, G., and Roy, J.-R. 1984*a*, *Pub. A.S.P.*, **96**, 263.
———. 1984*b*, *Ap. J.*, **283**, 640.
———. 1985, submitted.
Kaplan, S. A. 1966, *Interstellar Gas Dynamics* (New York: Pergamon).
Kaplan, S. A., and Pikel'ner, S. B. 1970, *The Interstellar Medium* (Cambridge: Harvard University Press).
Kennicutt, R. C. 1978, Ph.D. thesis, University of Washington.
———. 1979*a*, *Ap. J.*, **228**, 394.
———. 1979*b*, *Ap. J.*, **228**, 696.
———. 1979*c*, *Ap. J.*, **228**, 704.
———. 1981, *Ap. J.*, **247**, 9.
———. 1984, *Ap. J.*, **287**, 116.
Kolmogorov, A. N. 1941, *Dokl. Akad. Nauk SSSR*, **30**, 151.
Larson, R. B. 1979, *M.N.R.A.S.*, **186**, 479.
———. 1981, *M.N.R.A.S.*, **194**, 809.
Leung, L. M., Kutner, M. L., and Mead, K. N. 1982, *Ap. J.*, **262**, 583.
Lighthill, M. J. 1955, in *IAU Symposium 2, Gas Dynamics of Cosmic Clouds*, ed. H. C. van de Hulst and J. M. Burgers (Amsterdam: North-Holland), p. 121.
McCall, M. L. 1982, Ph.D. thesis, University of Texas at Austin.
McCall, M. L., Rybski, P. M., and Shields, G. A. 1985, *Ap. J. Suppl.*, **57**, 1.
Melnick, J. 1977, *Ap. J.*, **213**, 15.
———. 1978, *Astr. Ap.*, **70**, 157.
———. 1979, *Ap. J.*, **228**, 112.
———. 1980, *Astr. Ap.*, **86**, 304.
Münch, G. 1958, *Rev. Mod. Phys.*, **30**, 1035.
Myers, P. C. 1983, *Ap. J.*, **270**, 105.
Rayo, J. F., Peimbert, M., and Torres-Peimbert, S. 1982, *Ap. J.*, **255**, 1.
Richter, O. G., and Huchtmeier, W. K. 1984, *Astr. Ap.*, **132**, 253 (RH).
Rosa, M., and Solf, J. 1984, *Astr. Ap.*, **130**, 29.
Roy, J.-R., and Joncas, G. 1985, *Ap. J.*, **288**, 142.
Sabbadin, F., Ortolani, S., and Bianchini, A. 1985, *M.N.R.A.S.*, **213**, 563.
Sandage, A. 1962, in *IAU Symposium 15, Problems of Extragalactic Research*, ed. G. C. McVittie (New York: Macmillan), p. 359.
Sandage, A., and Tammann, G. A. 1974, *Ap. J.*, **190**, 525.
———. 1981, *A Revised Shapley-Ames Catalog of Bright Galaxies* (Washington: Carnegie Institution of Washington).
———. 1982, *Ap. J.*, **256**, 339.
Scalo, J. M. 1984, *Ap. J.*, **277**, 557.
Sérsic, J. L. 1960, *Zs. Ap.*, **50**, 168.
Skillman, E. D., and Balick, B. 1984, *Ap. J.*, **280**, 580.
Smith, M. G., and Weedman, D. W. 1970, *Ap. J.*, **161**, 33.
———. 1972, *Ap. J.*, **172**, 307.
Stasińska, G., Alloin, D., Collin-Souffrin, S., and Joly, M. 1981, *Astr. Ap.*, **93**, 362.
Stenholm, L. G. 1984, *Astr. Ap.*, **137**, 133.
Teerikorpi, P. 1985, *Astr. Ap.*, **143**, 469.
Tennekes, H., and Lumley, J. L. 1972, *A First Course in Turbulence* (Cambridge: MIT Press).
Tenorio-Tagle, G. 1979, *Astr. Ap.*, **71**, 59.
Terlevich, R., and Melnick, J. 1981, *M.N.R.A.S.*, **195**, 839.
Tully, R. B., and Fisher, J. R. 1977, *Astr. Ap.*, **54**, 661.
von Hoerner, S. 1951, *Zs. Ap.*, **30**, 17.
von Weizsäcker, C. F. 1951, *Ap. J.*, **114**, 165.

ROBIN ARSENAULT and JEAN-RENÉ ROY: Département de physique, Université Laval, Québec, Qc G1K 7P4, Canada

GILLES JONCAS: Observatoire de Marseille, 2 Place le Verrier, 13248 Marseille, Cedex 4, France